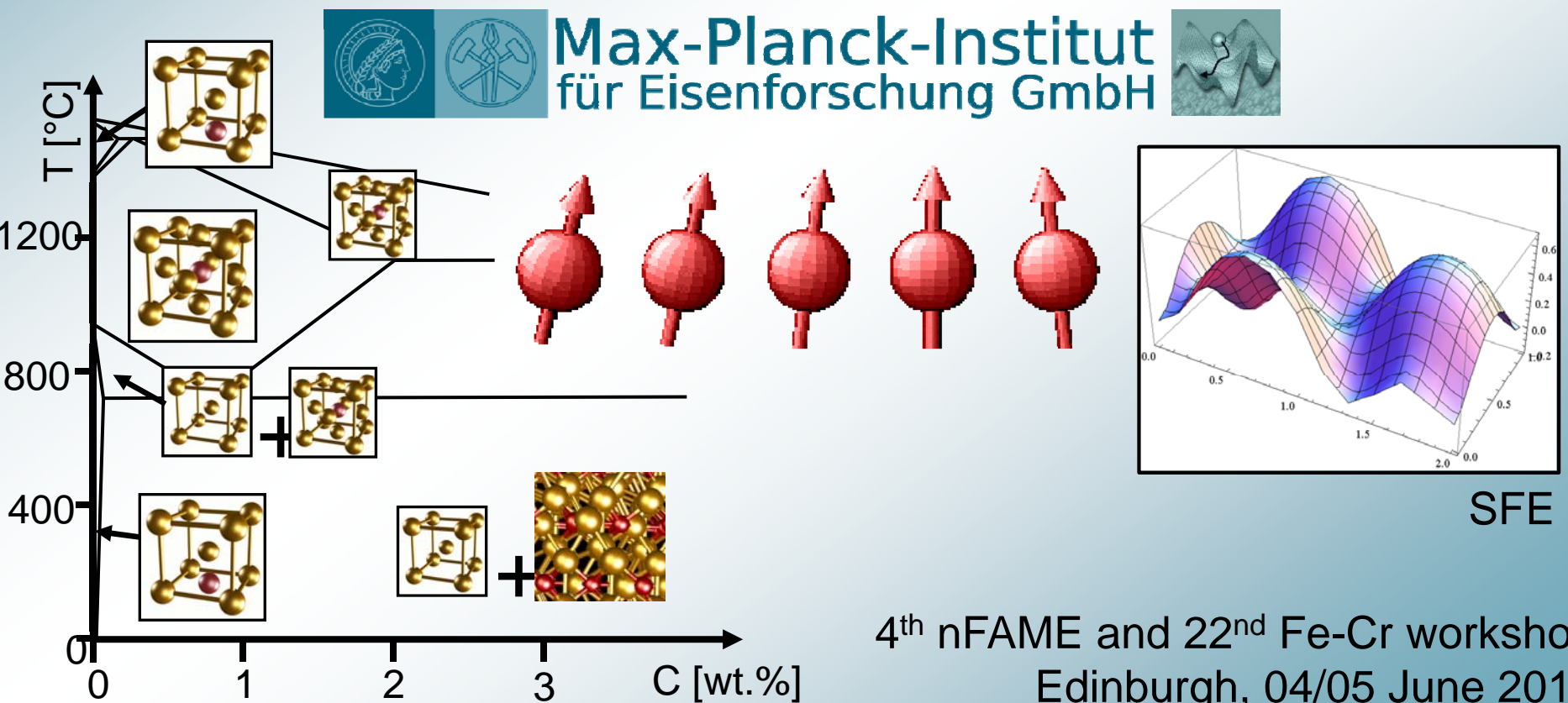
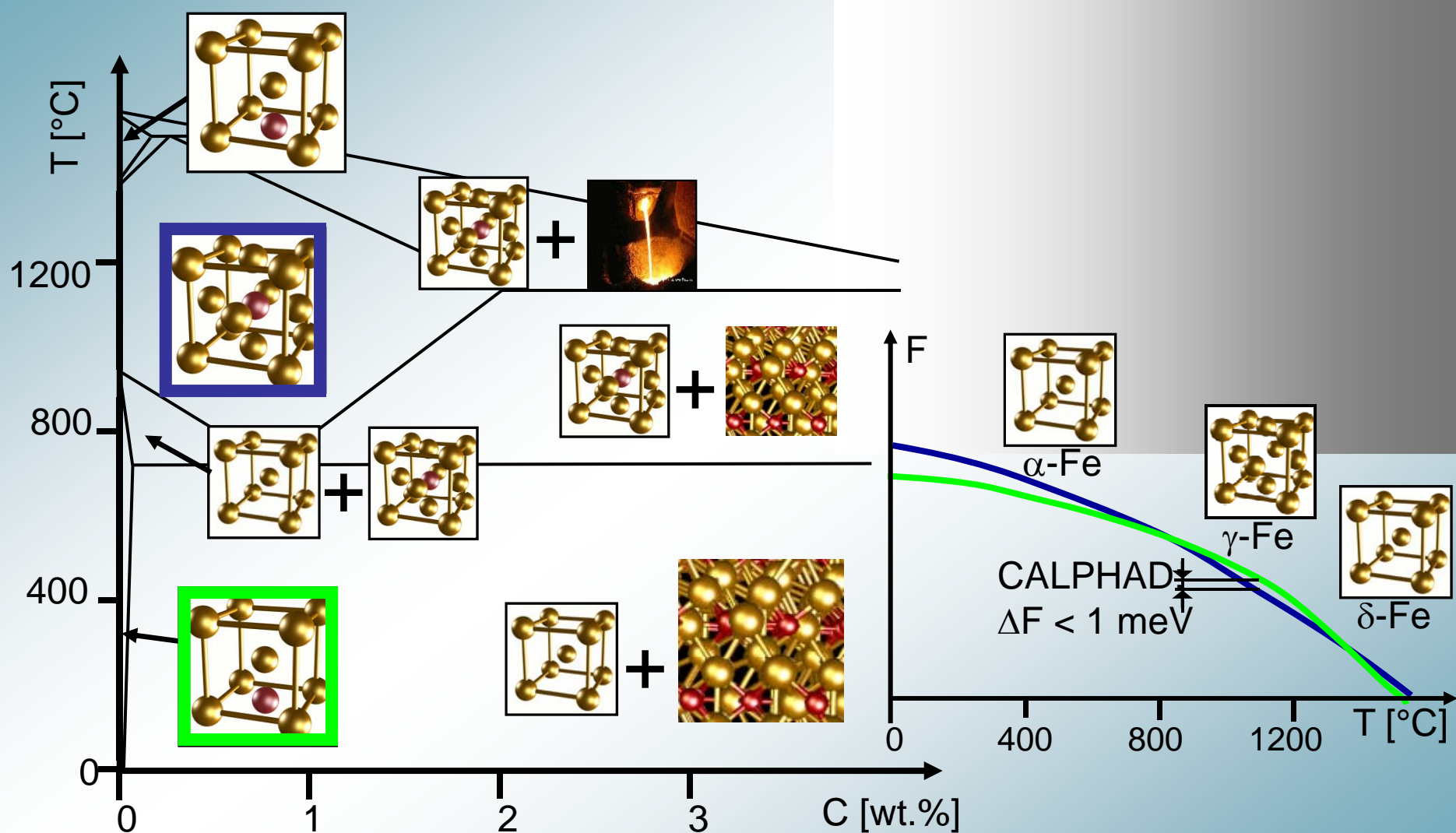


Ab initio investigation of austenitic steels: The interplay of composition, magnetism and mechanical behaviour

Tilmann Hickel, F. Körmann, I. Bleskov, J. Neugebauer

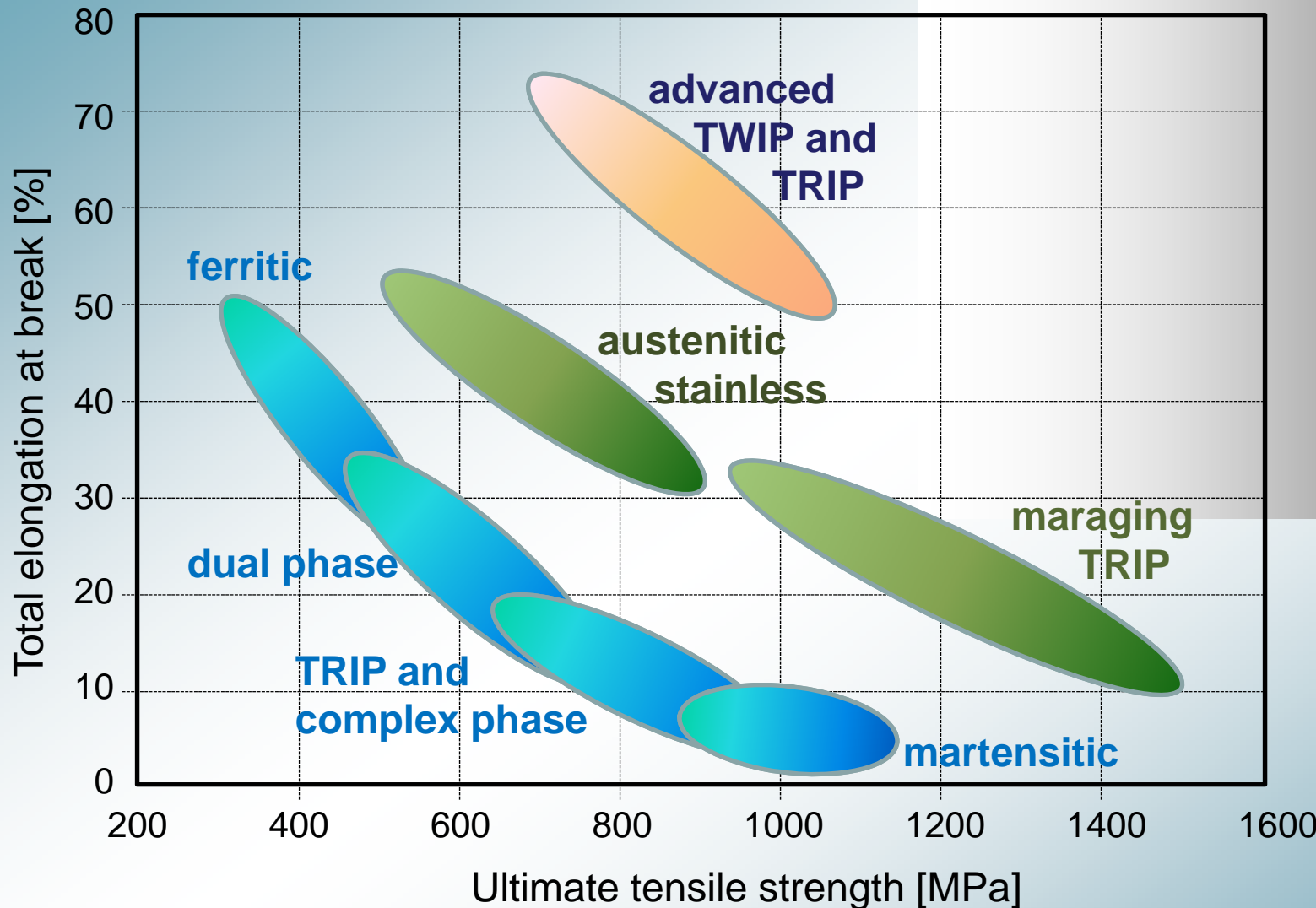


Phase diagrams: The Fe-C system

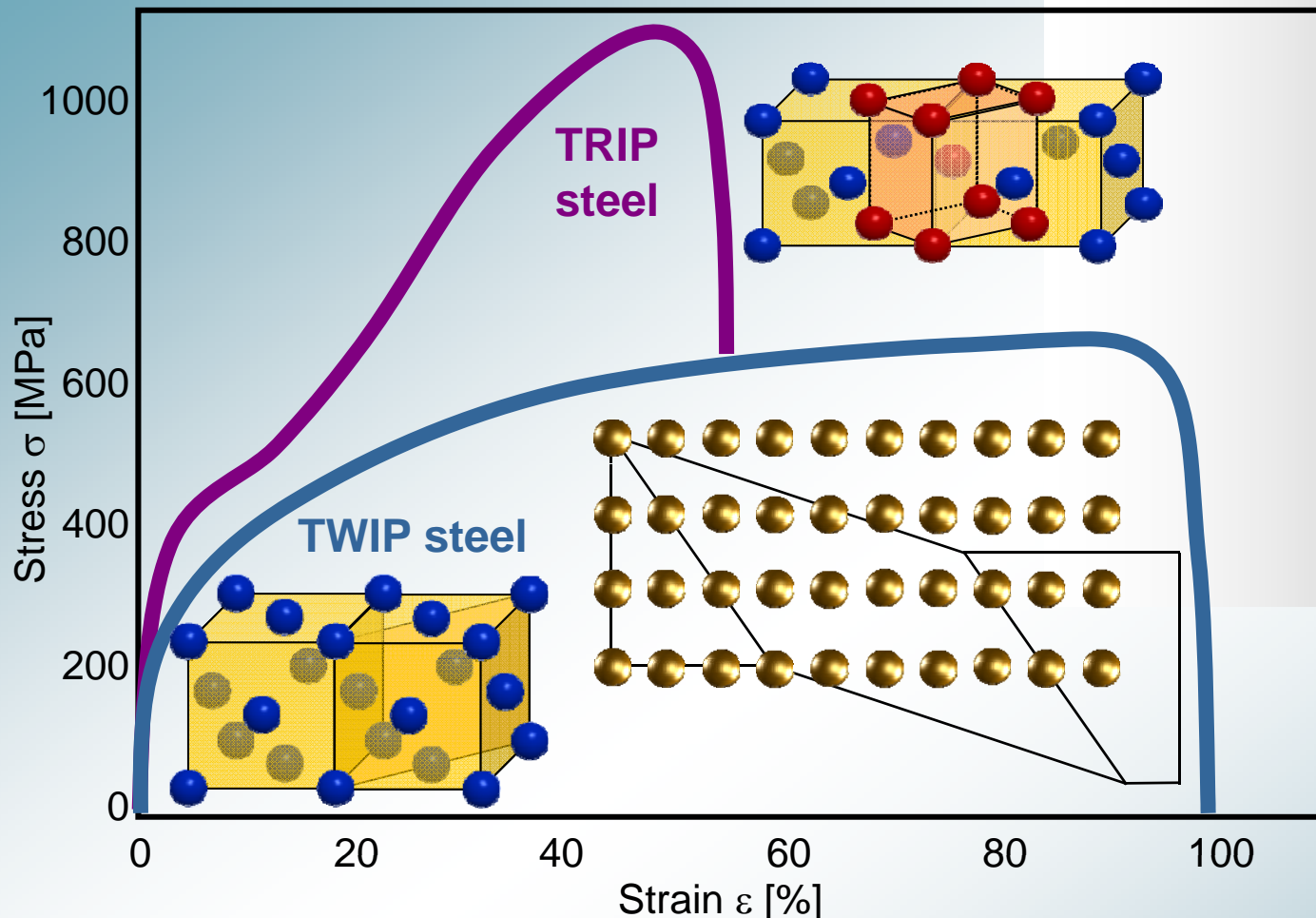


- accuracy 1000x smaller than typical binding energies required

Materials design for innovative steels



Materials design for innovative steels



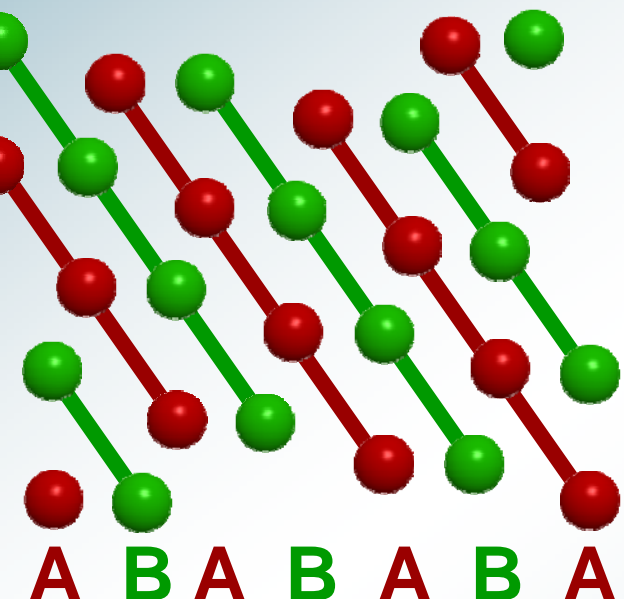
- deformation processes in innovative steels: TRIP and TWIP
- controlled by stacking fault energy
- based on free energy calculations

Stacking sequences

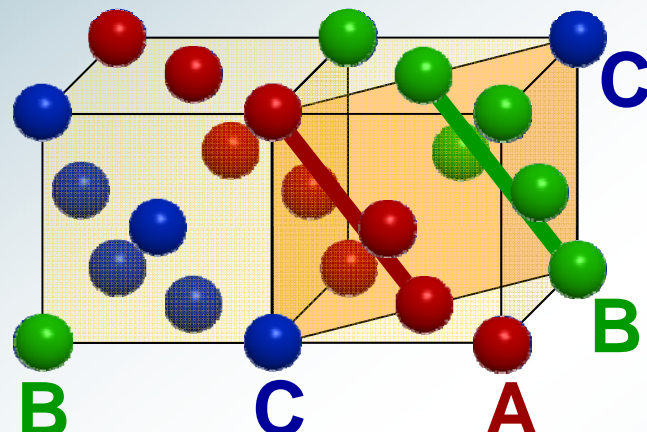
TRIP

phase transformation

$$\gamma \rightarrow \varepsilon \rightarrow \alpha'$$



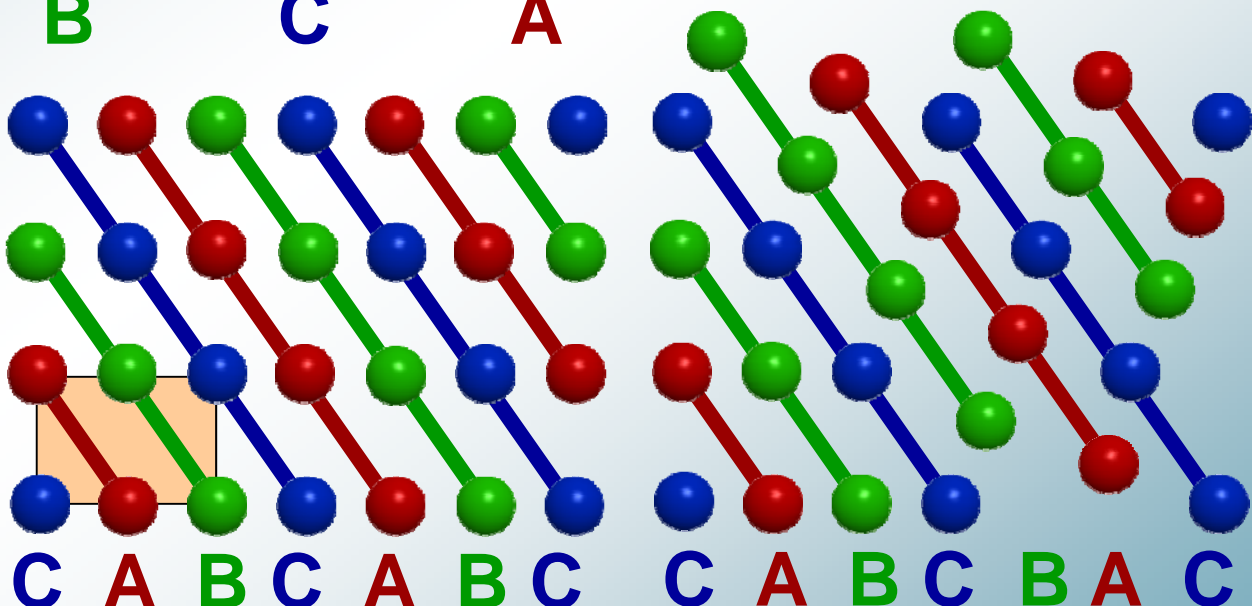
Austenite



TWIP

twinning formation

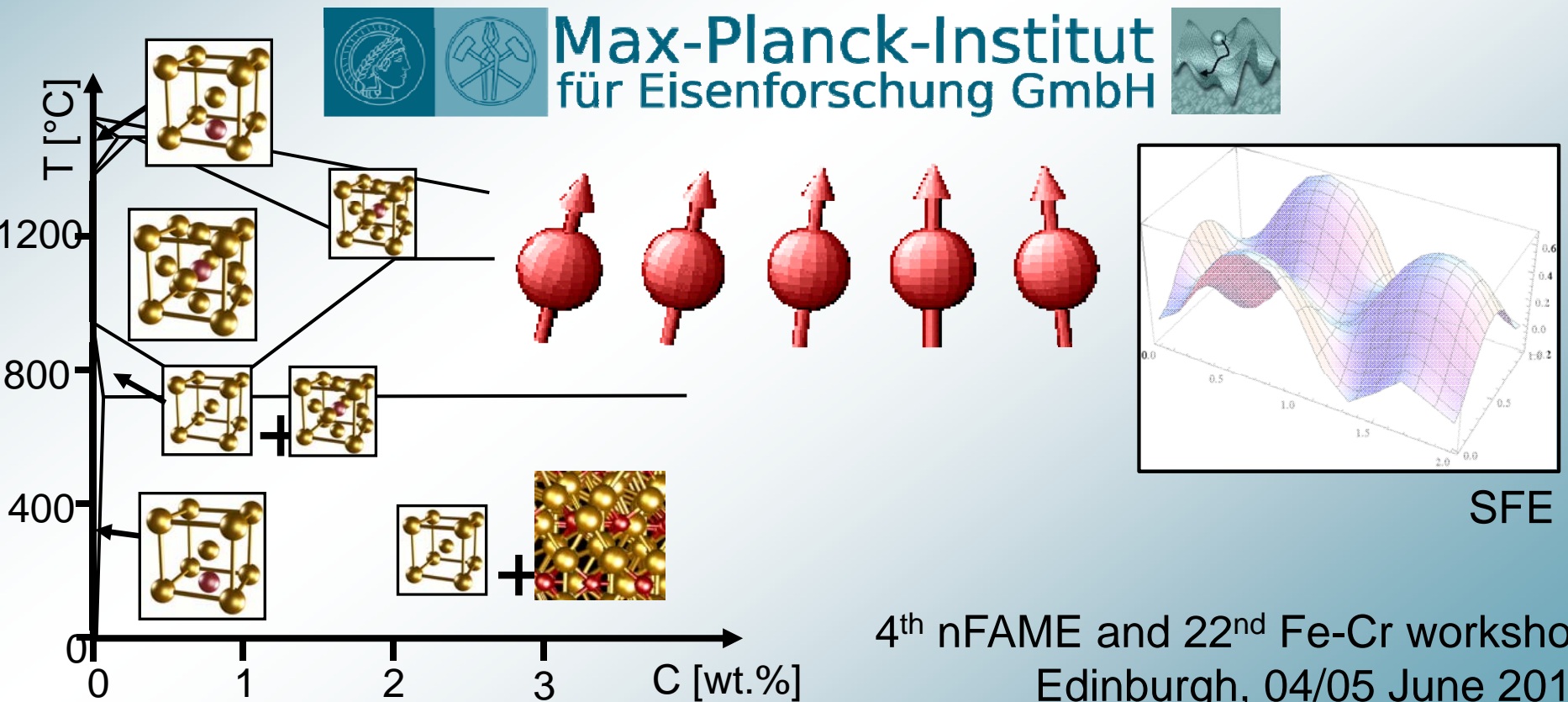
Σ_3 twin boundaries



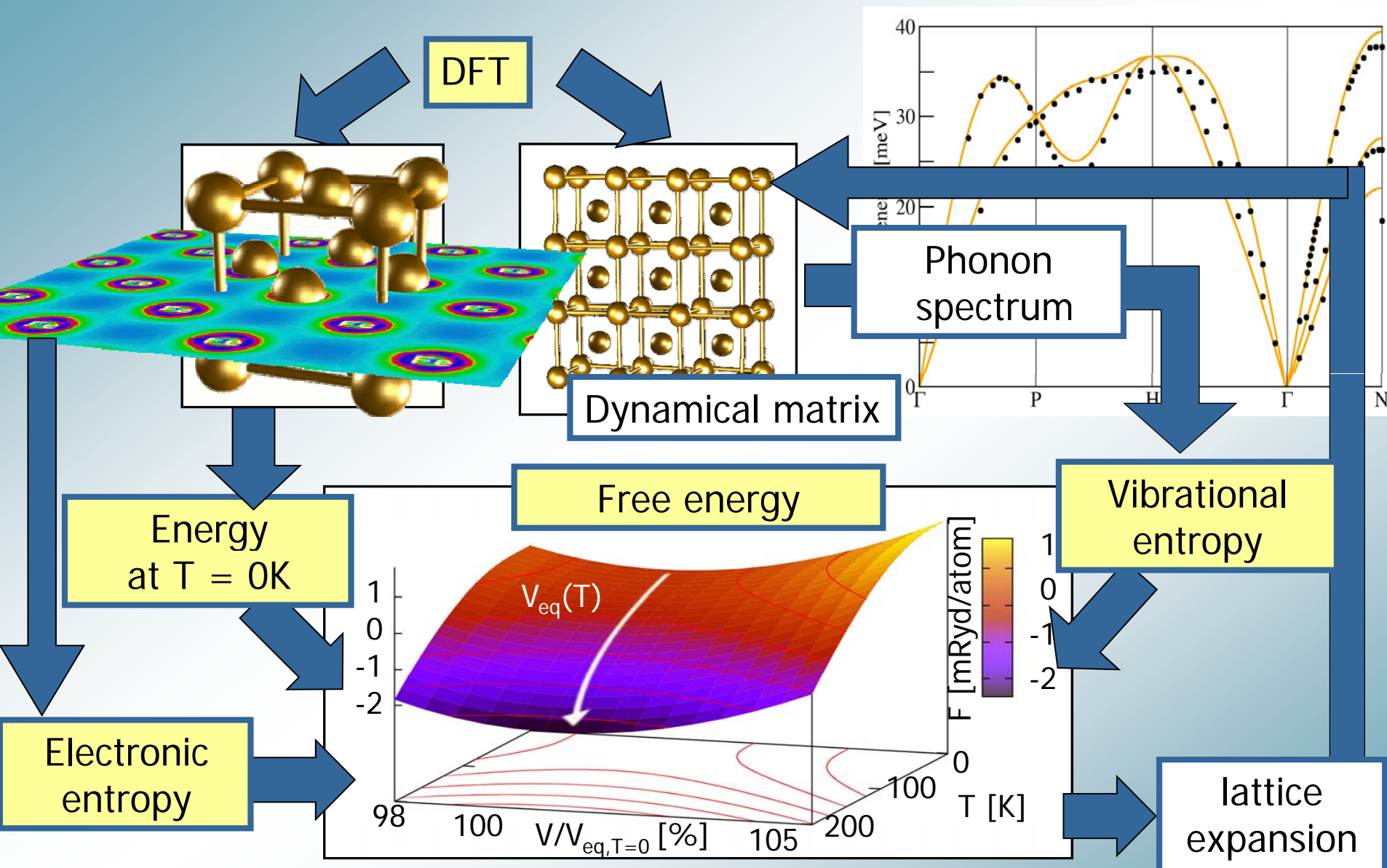
- stacking faults are decisive for mechanical behaviour
- stacking fault energy (SFE) determines importance of TRIP, TWIP

Ab initio investigation of austenitic steels: The interplay of composition, magnetism and mechanical behaviour

Tilmann Hickel, F. Körmann, I. Bleskov, J. Neugebauer



Ab initio for finite temperatures

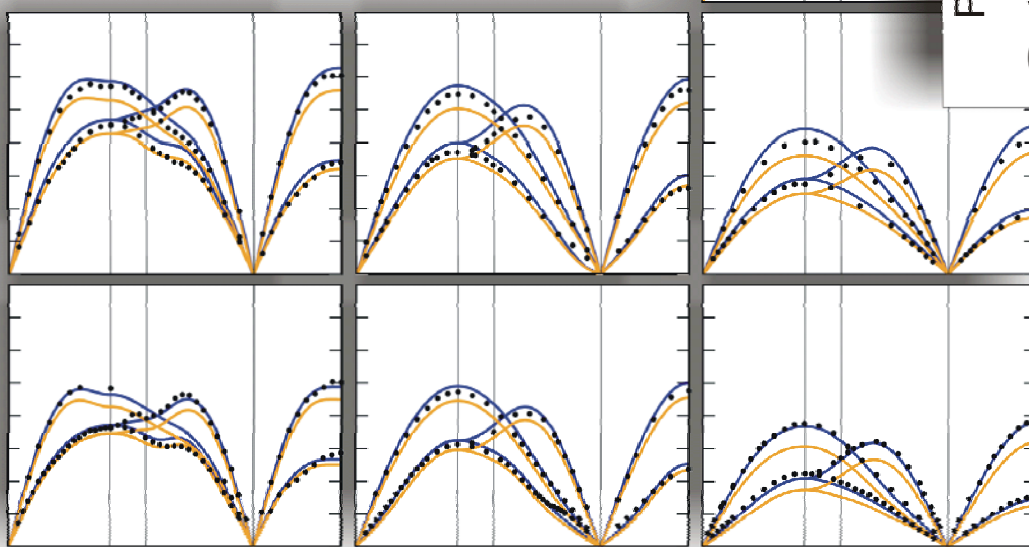
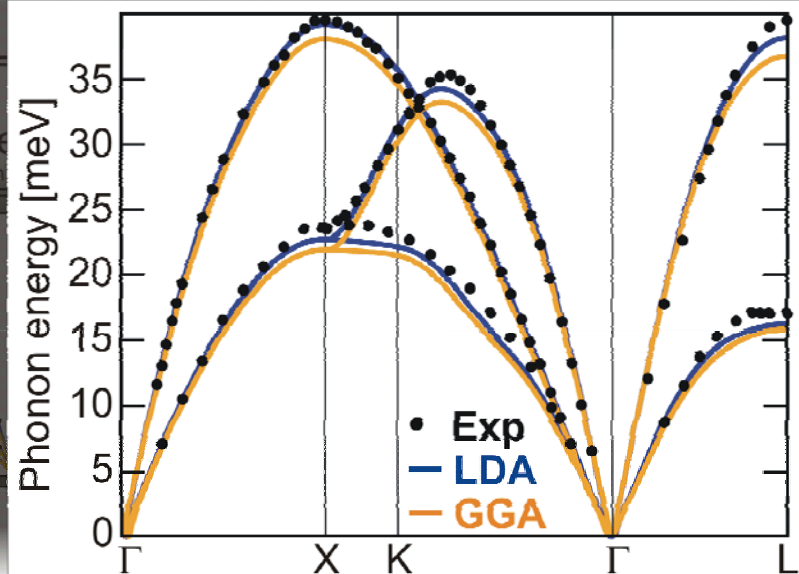




Performance for phonon energies

Mn Manganese	55.85 [Ar]3d ⁵ 4s ²	58.93 [Ar]3d ⁵ 4s ²	58.69 [Ar]3d ⁵ 4s ²	63.55 [Ar]3d ¹⁰ 4s	65.39 [Ar]3d ¹⁰ 4s ²	69.72 [Zn]4p ²	72.64 [Zn]4p ²
Fe Iron	26Fe Iron	27Co Cobalt	28Ni Nickel	29Cu Copper	30Zn Zinc	31Ga Gallium	32Ge Germanium
Tc Tc medium	101.07 [Kr]4d ⁵ 5s	102.91 [Kr]4d ⁵ 5s	106.42 [Kr]4d ¹⁰	107.87 [Kr]4d ¹⁰ 5s	112.41 [Kr]4d ¹⁰ 5s ²	144.92 [Zn]4p ²	149.74 [Zn]4p ²
Ru Ruthenium	44Ru Ruthenium	45Rh Rhodium	46Pd Palladium	47Ag Silver	48Cd Cadmium	50Cd Cadmium	52Ge Germanium
Os Osmium	190.23 [Xe]4f ¹ 5d ⁷ 6s ²	192.22 [Xe]4f ¹ 5d ⁷ 6s ²	195.08 [Xe]4f ¹ 5d ⁷ 6s	196.97 [Xe]4f ¹ 5d ⁷ 6s ²	200.59 [Xe]4f ¹ 5d ⁷ 6s ²	204.71 [Xe]4f ¹ 5d ⁷ 6s ²	207.71 [Xe]4f ¹ 5d ⁷ 6s ²
Ir Iridium	76Os Osmium	77Ir Iridium	78Pt Platinum	79Au Gold	80Hg Mercury	82Hg Mercury	84Ge Germanium

10.81 [He]2s ² 2p	12.01 [He]2s ² 2p ²	14.01 [He]2s ² 2p ³	16.00 [He]2s ² 2p ⁴
B Boron	C Carbon	N Nitrogen	O Oxygen
26.98 [Ne]3s ² 3p	28.09 [Ne]3s ² 3p ²	30.97 [Ne]3s ² 3p ³	32.07 [Ne]3s ² 3p ⁴
Al Aluminum	Si Silicon	P Phosphorus	S Sulfur



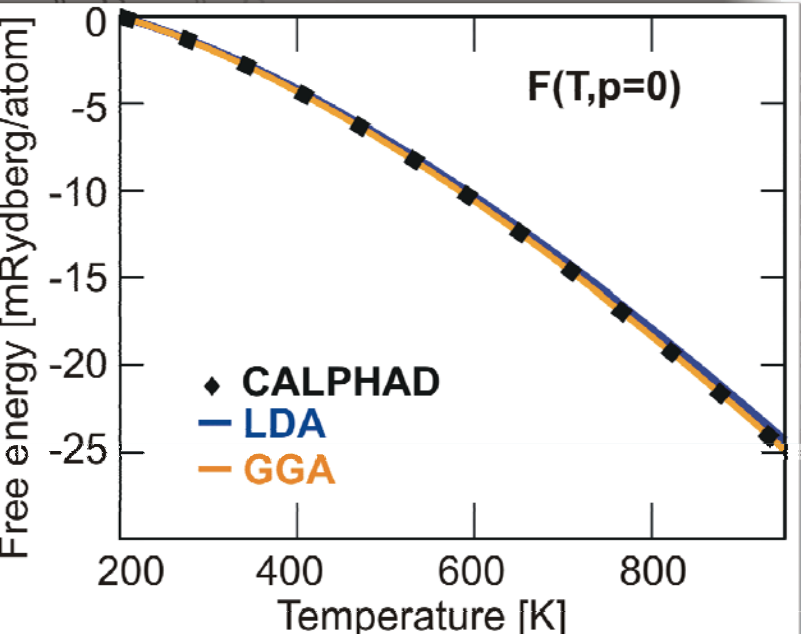
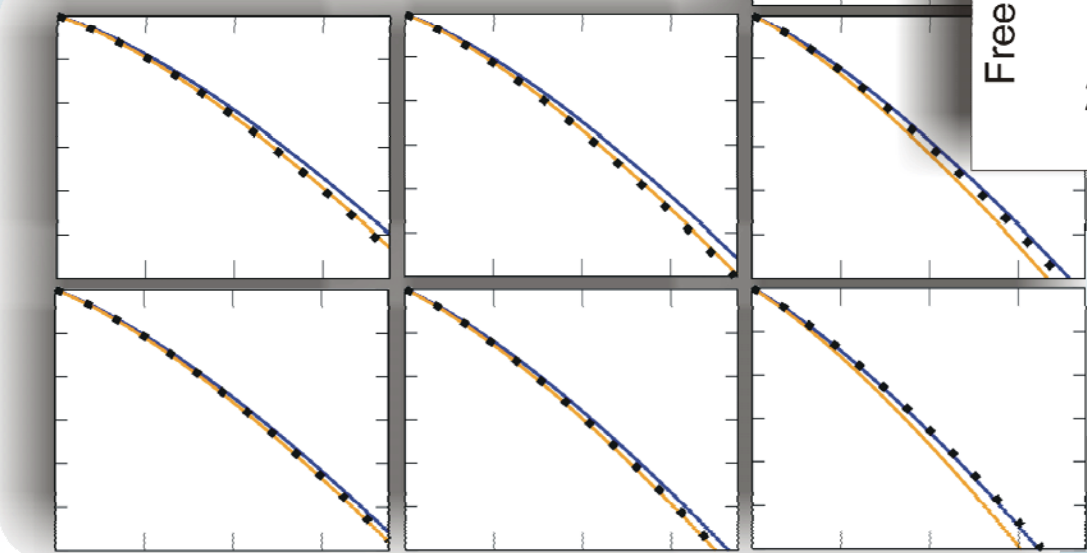
- Phonon energies with reasonable accuracy
- Differences of XC-functionals indicate predictive power



Performance for free energies

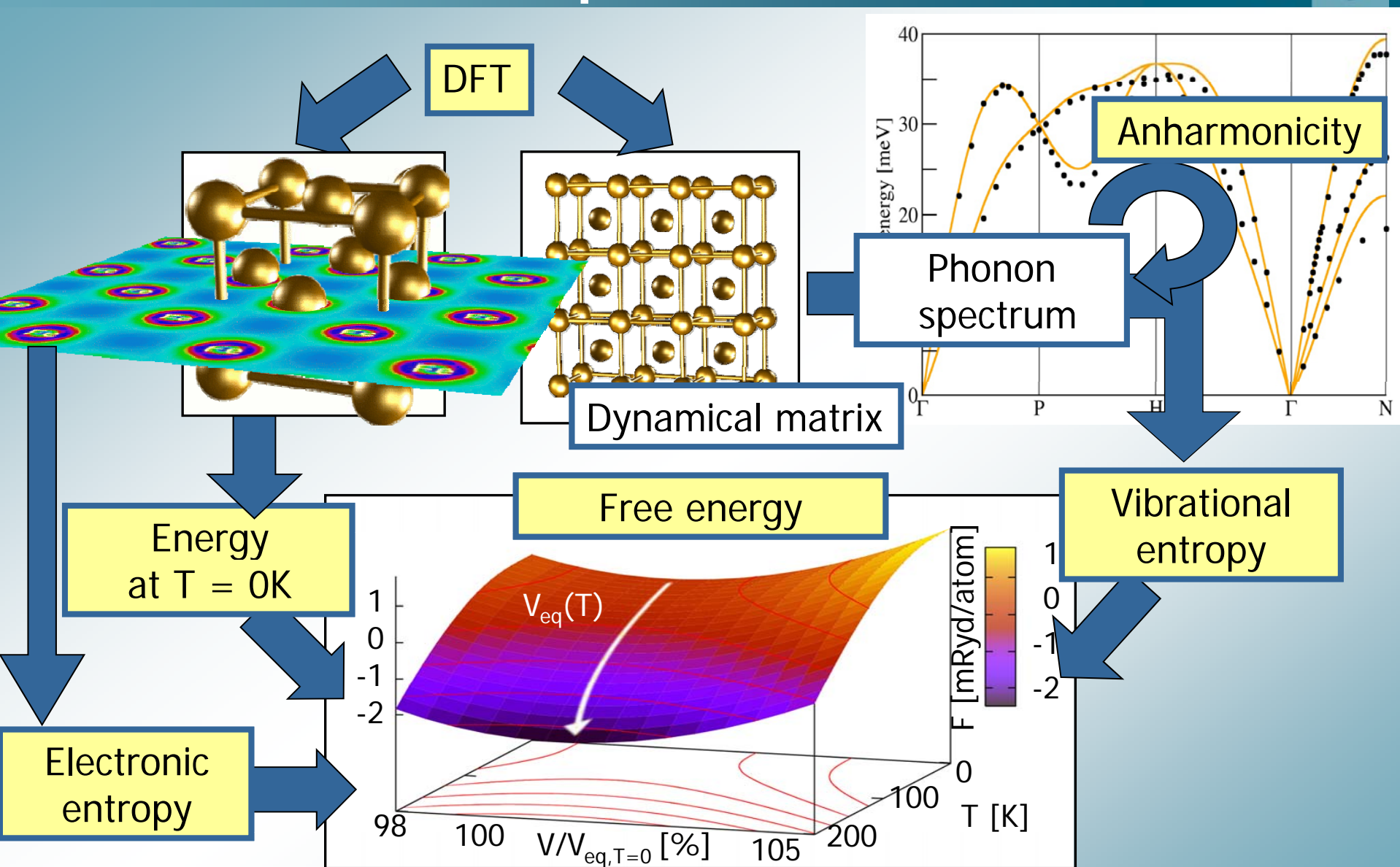
14 3d ⁵ 4s ² Mn transition metals	55.85 [Ar]3d ⁵ 4s ² 26Fe Iron	58.93 [Ar]3d ⁵ 4s ² 27Co Cobalt	58.69 [Ar]3d ⁵ 4s ² 28Ni Nickel	63.55 [Ar]3d ¹⁰ 4s 29Cu Copper	65.39 [Ar]3d ¹⁰ 4s ² 30Zn Zinc	69.72 [Zn]4p 31Ga Gallium	72.64 [Zn]4p 32Ge Germanium
51 4d ⁵ 5s Tc transition metals	101.07 [Kr]4d ⁵ 5s 44Ru Ruthenium	102.91 [Kr]4d ⁵ 5s 45Rh Rhodium	106.42 [Kr]4d ¹⁰ 46Pd Palladium	107.87 [Kr]4d ¹⁰ 5s 47Ag Silver	112.41 [Kr]4d ¹⁰ 5s ² 48Cd Cadmium	114.92 [Kr]4d ¹⁰ 5s ² 50Zn Zinc	119.71 [Kr]4d ¹⁰ 5s ² 51Ga Gallium
71 4f ¹³ 5d ¹⁰ 6s ² Re transition metals	190.23 [Xe]4f ¹³ 5d ¹⁰ 6s ² 76Os Osmium	192.22 [Xe]4f ¹³ 5d ¹⁰ 6s ² 77Ir Iridium	195.08 [Xe]4f ¹³ 5d ¹⁰ 6s 78Pt Platinum	196.97 [Xe]4f ¹³ 5d ¹⁰ 6s 79Au Gold	200.59 [Xe]4f ¹³ 5d ¹⁰ 6s 80Hg Mercury		

10.81 [He]2s ² 2p 5B Boron	12.01 [He]2s ² 2p ² 6C Carbon	14.01 [He]2s ² 2p ⁴ 7N Nitrogen	16.00 [He]2s ² 2p ⁵ 8O Oxygen
26.98 [Ne]3s ² 3p 13Al Aluminum	28.09 [Ne]3s ² 3p ² 14Si Silicon	30.97 [Ne]3s ² 3p ³ 15P Phosphorus	32.07 [Ne]3s ² 3p ⁴ 16S Sulfur

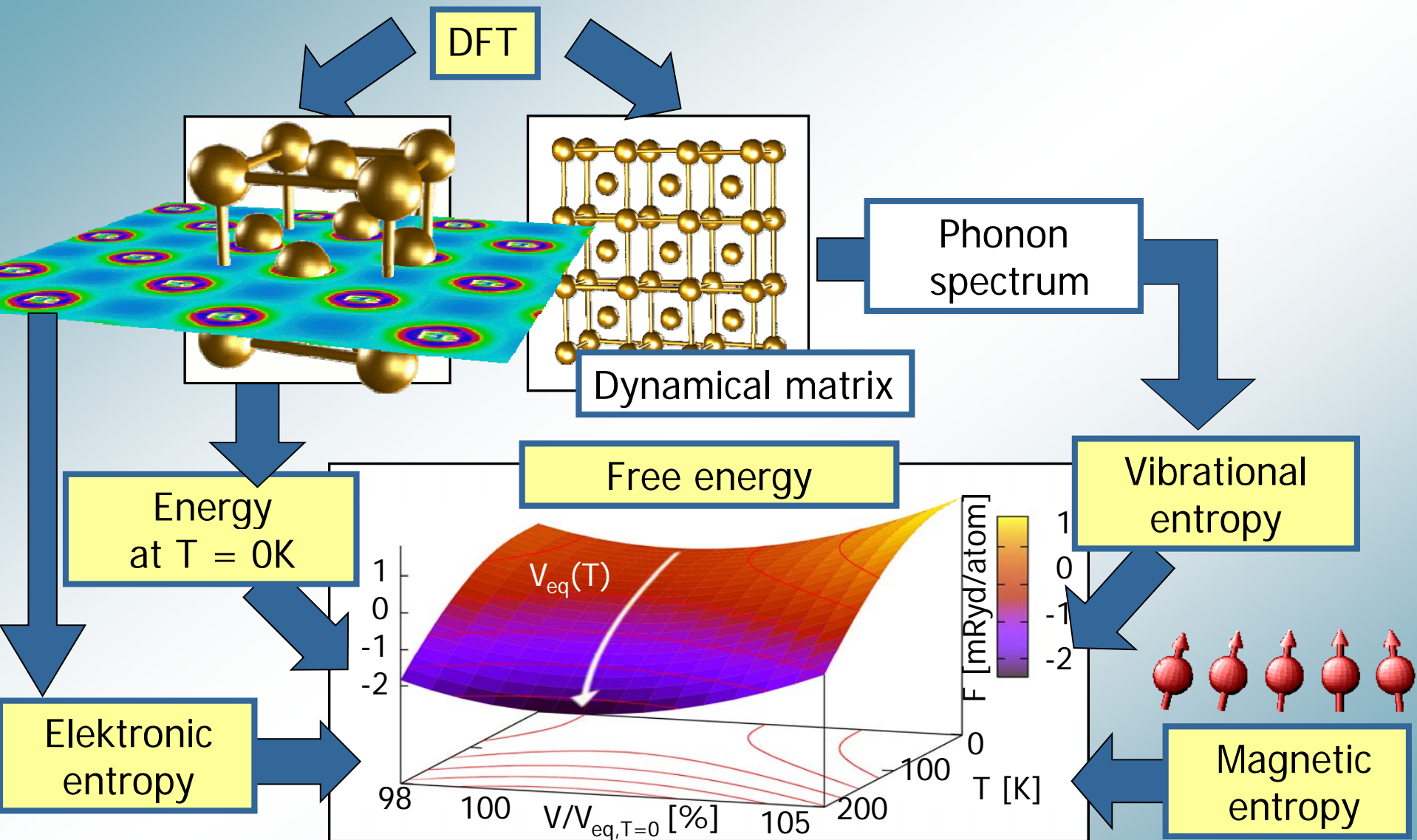


➤ Accuracy of derived free energies sufficient for many materials

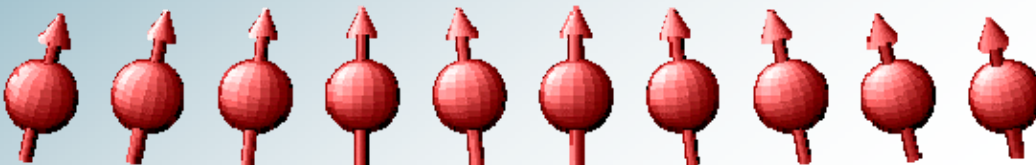
Ab initio for finite temperatures



Ab initio for finite temperatures



Treatment of magnetic excitations



- DFT for magnons

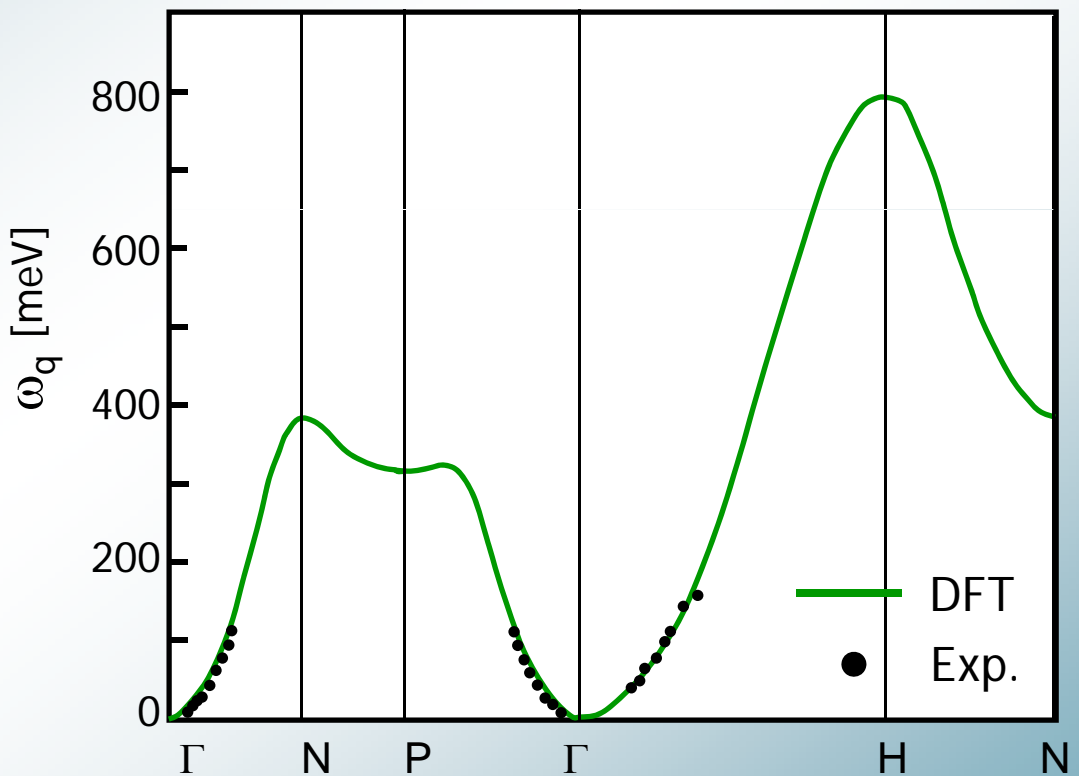
$$\omega_q = \frac{4}{M} \lim_{\theta \rightarrow 0} \frac{\Delta E(q, \theta)}{\sin^2 \theta}$$

- calculated and measured magnons in good agreement

$$H = - \sum_{i,j} J_{i,j} \mathbf{S}_i \cdot \mathbf{S}_j$$

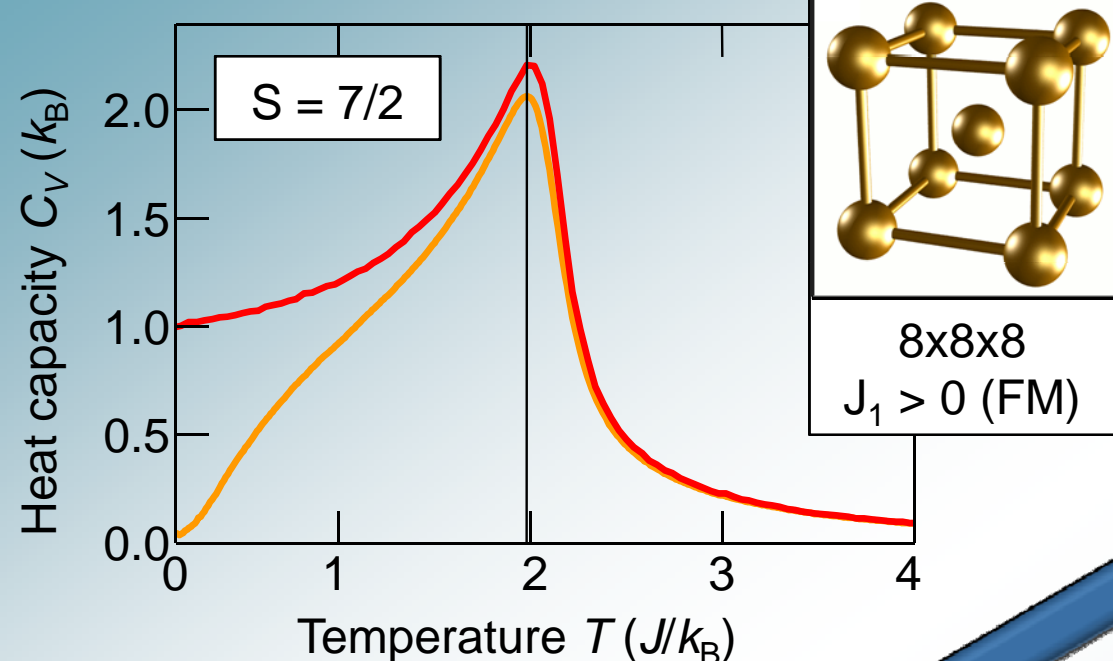
- exchange integrals derived from magnon spectrum

$$\omega_q = \frac{4}{M} (J_0 - J_q)$$



J. Lynn, PRB **11**, 2624 (1974).
 C. Loong et al., JAP **55**, 1895 (1984).

Simulation of Heisenberg model systems



- well defined (finite size) crystal structure
- only nearest-neighbor magnetic interaction

$$H = - \sum_{ij} J_{ij} \hat{S}_i \hat{S}_j$$

Quantum solution

\hat{S}_j operators

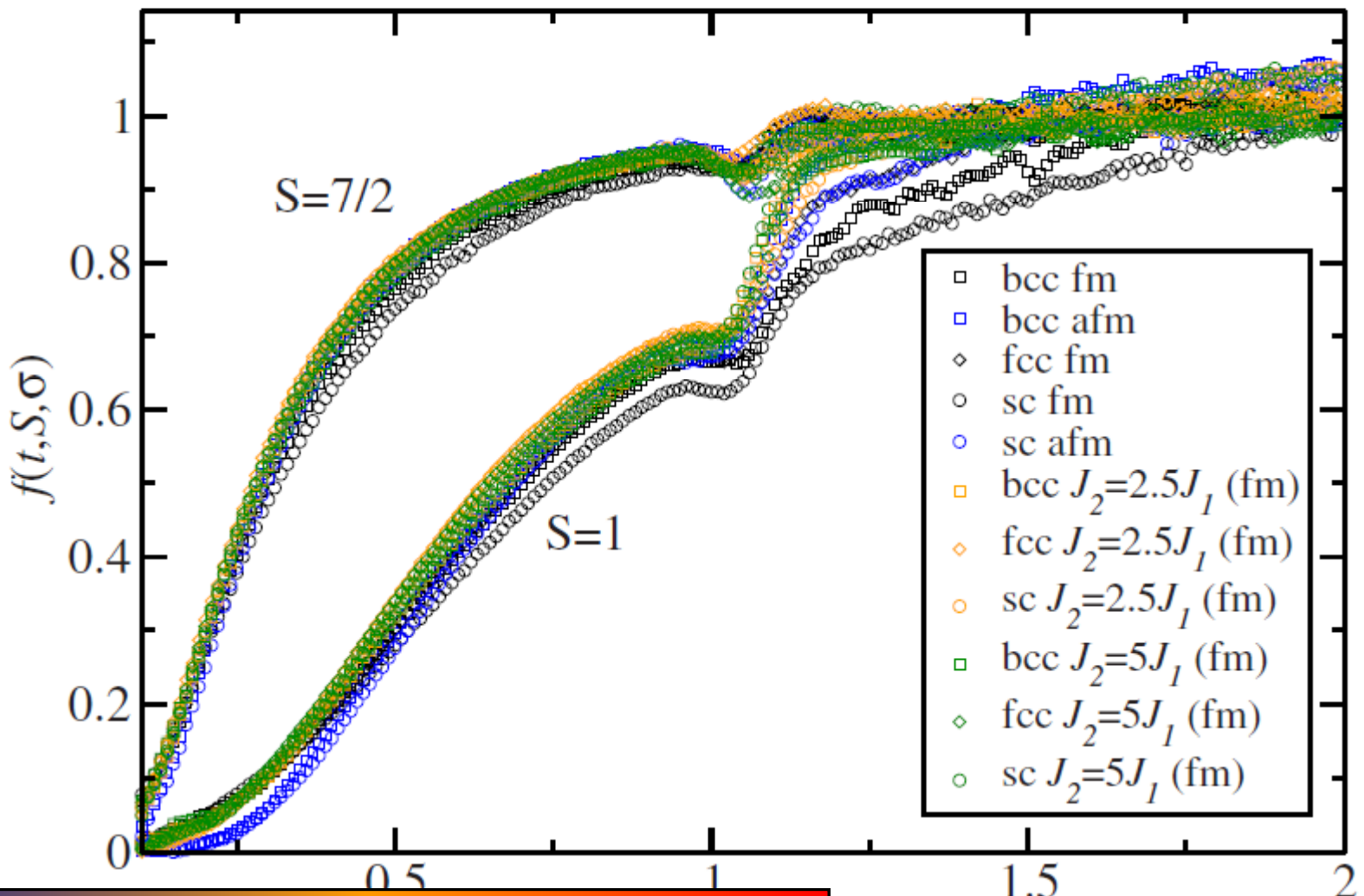
$$\langle A \rangle_{QM} = \text{Tr} \left\{ A e^{-\beta H} \right\} / \text{Tr} \left\{ e^{-\beta H} \right\}$$

Classical solution

\hat{S}_j continuous vectors

$$\langle A \rangle_{CL} = \sum_c A_c e^{-\beta E_c} / \sum_c e^{-\beta E_c}$$

Analysis of different MC approaches



$$f(t, S, \sigma) = C_V^{qm}(t, S) / C_V^{cl}(t)$$

Magnetic entropy for bcc iron

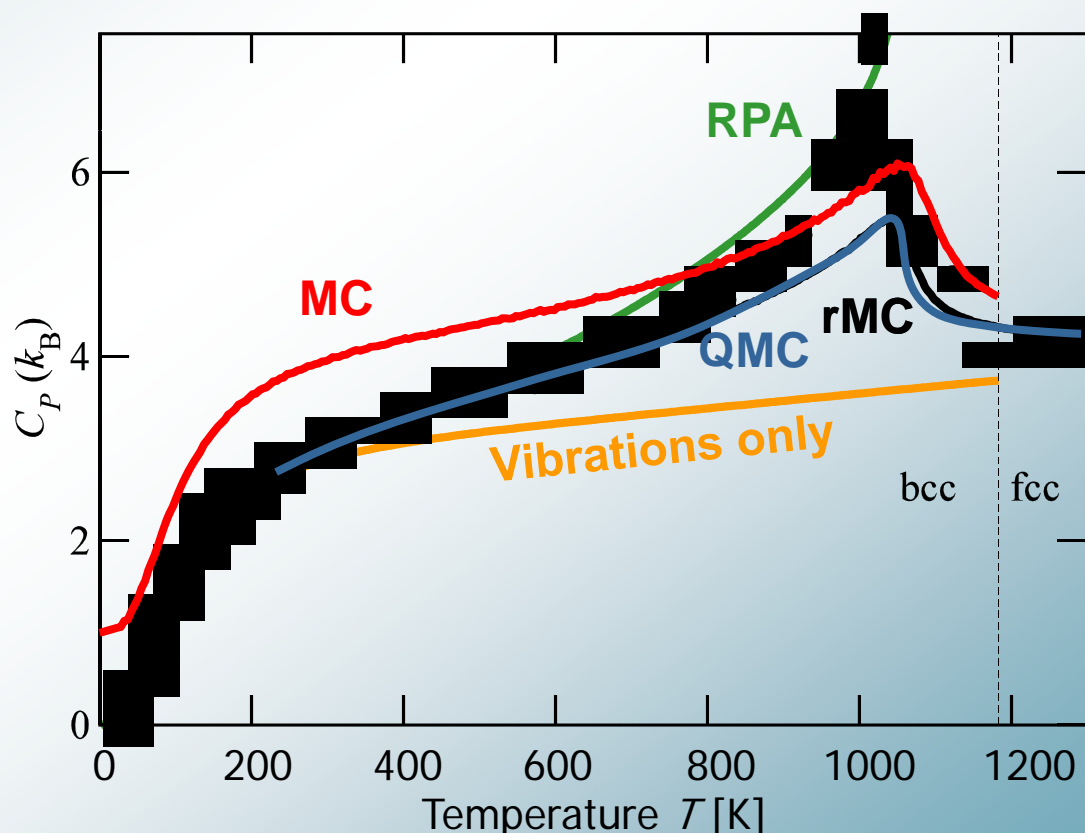
Magnetic entropy important contribution to free energy of bcc iron

Shortcomings of approaches:

- analytical approach (**RPA**): cannot cover complete temperature range
- classical Monte-Carlo (**MC**): error at low temperatures due to quantum effects
- quantum Monte-Carlo (**rMC**): negative sign problem

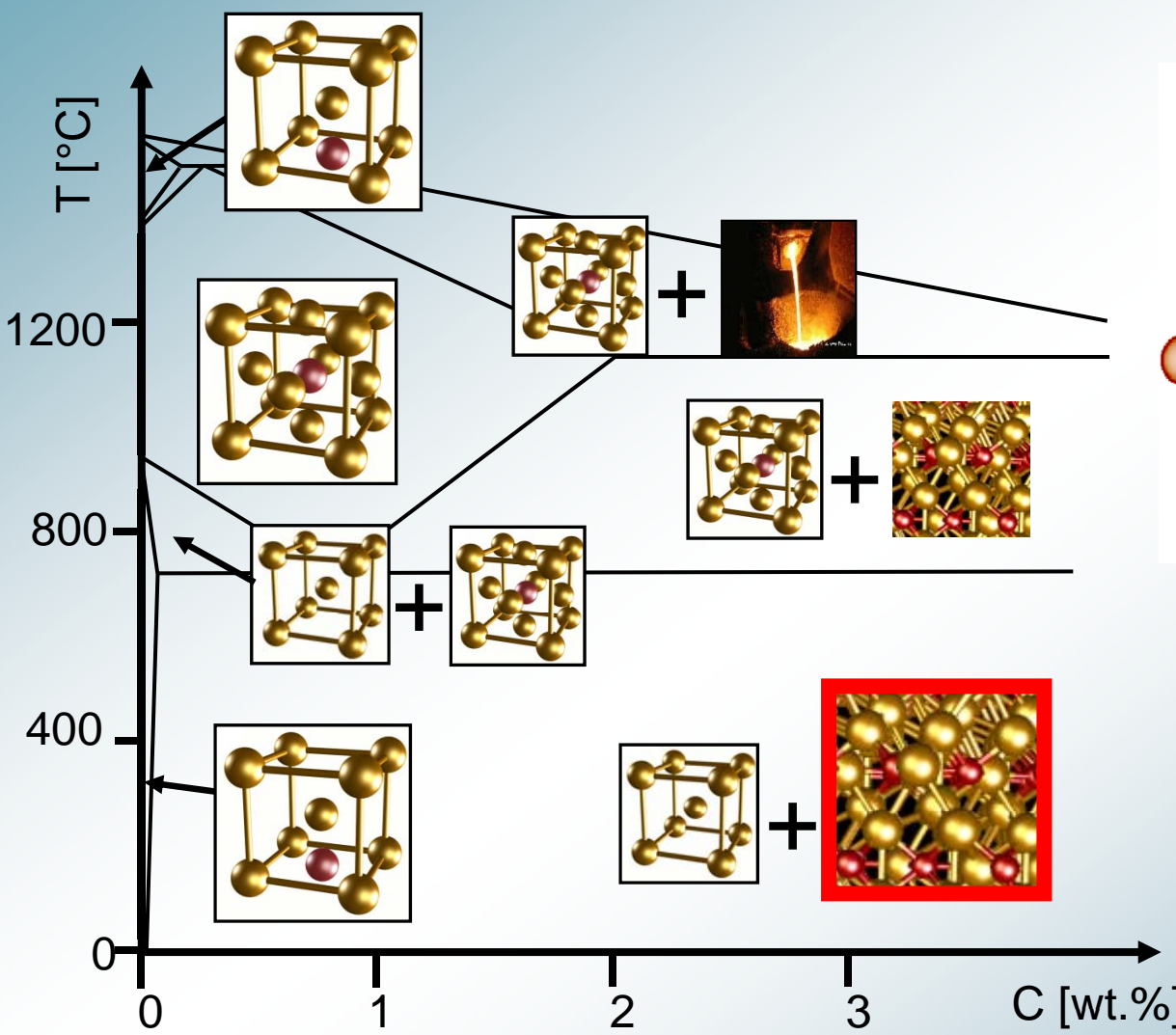
Effective nn approach (QMC):

- Define an effective Heisenberg model with only nearest-neighbor interactions
- Ensure the correct critical temperature
- Perform QMC calculations for this model
- Derive free energy by integration down from the exact high-temperature limit

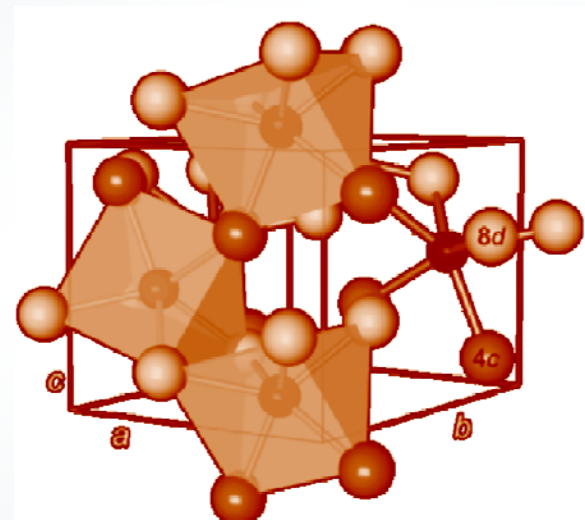


Numerics performed with ALPS simulation package.

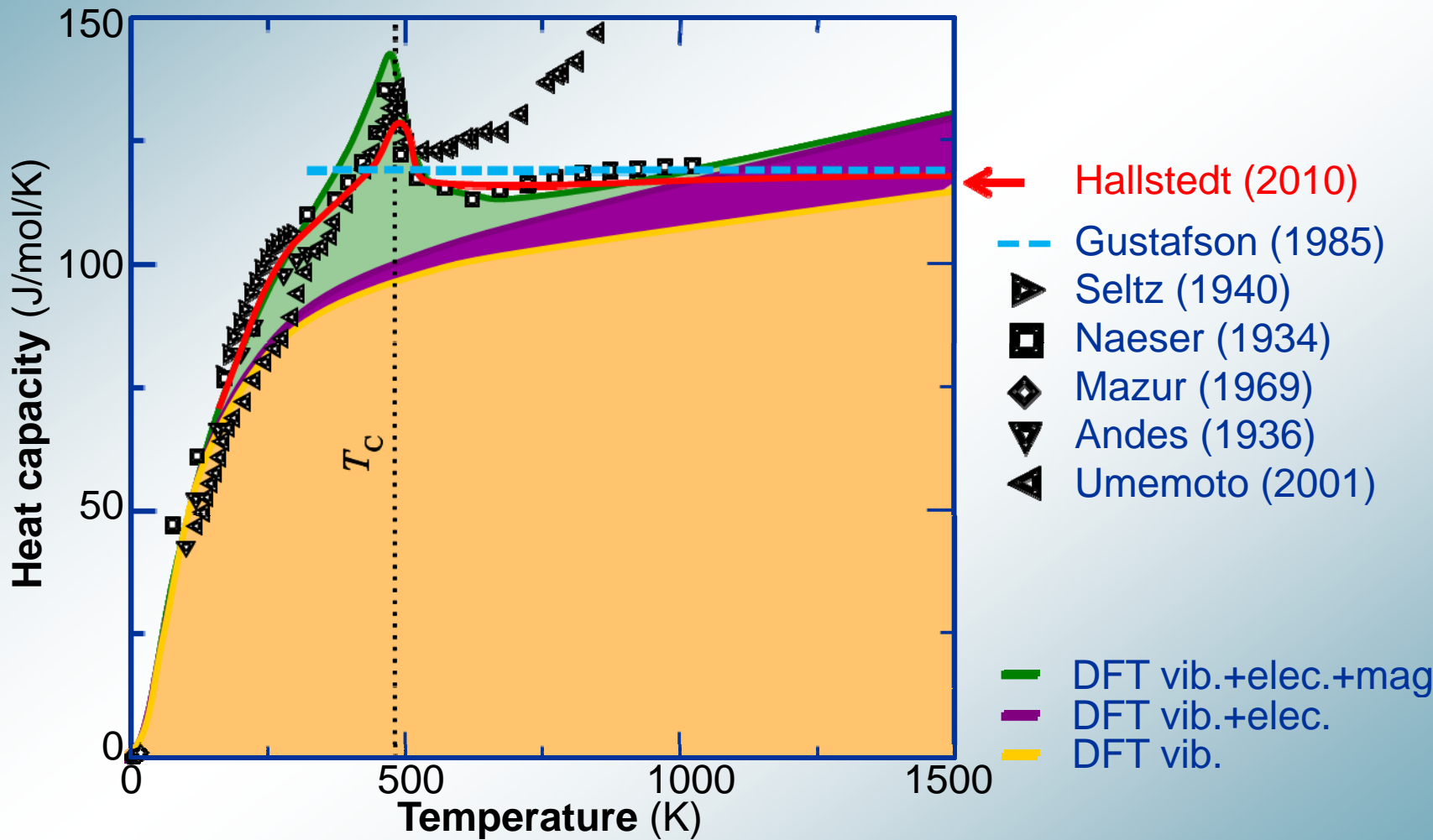
The Fe-C system



Cementite Fe_3C



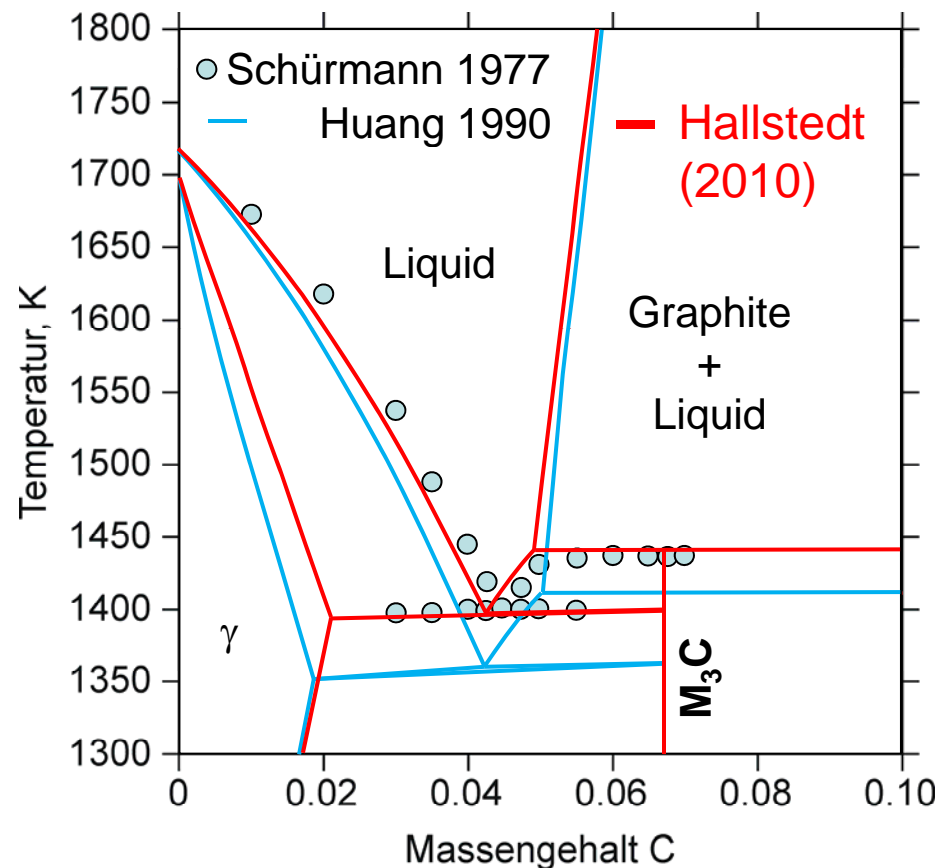
Heat capacity of Fe_3C



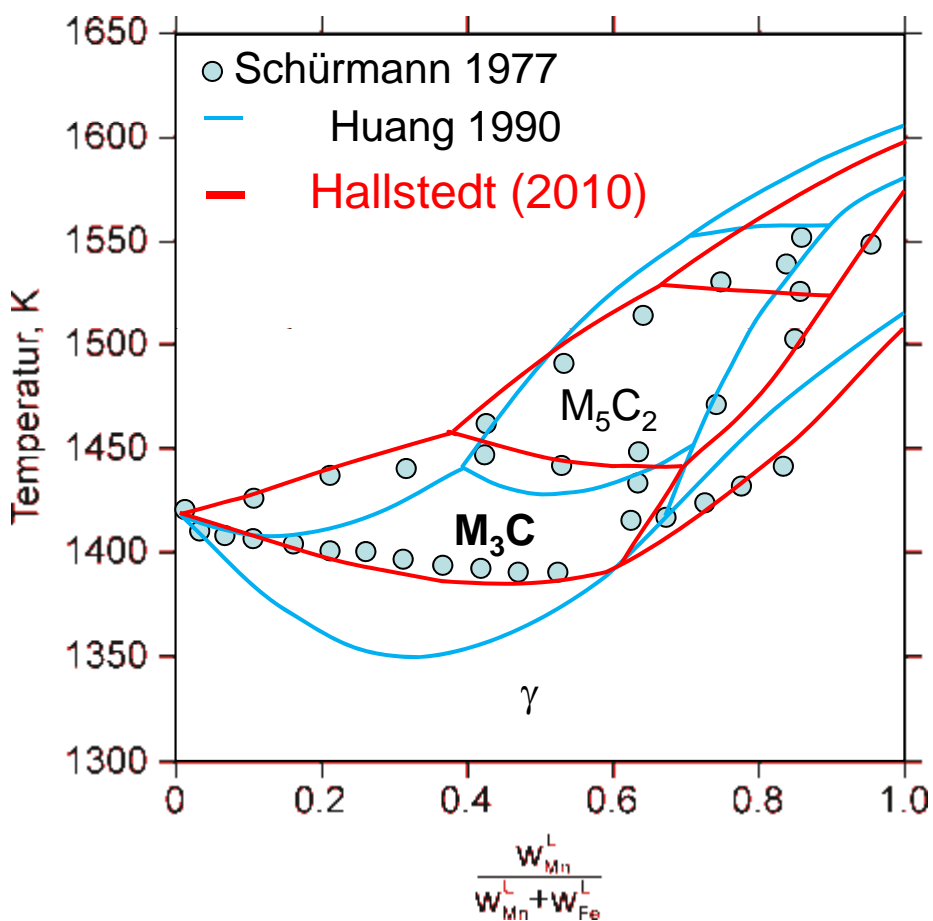
B. Hallstedt, D. Djurovic, J. von Appen, R. Dronskowski, A. Dick, F. Körmann, T. Hickel, J. Neugebauer, *Calphad*, **34**, 129 (2010).

Relevance for phase diagram

Phase diagram isopleth for 20% Mn

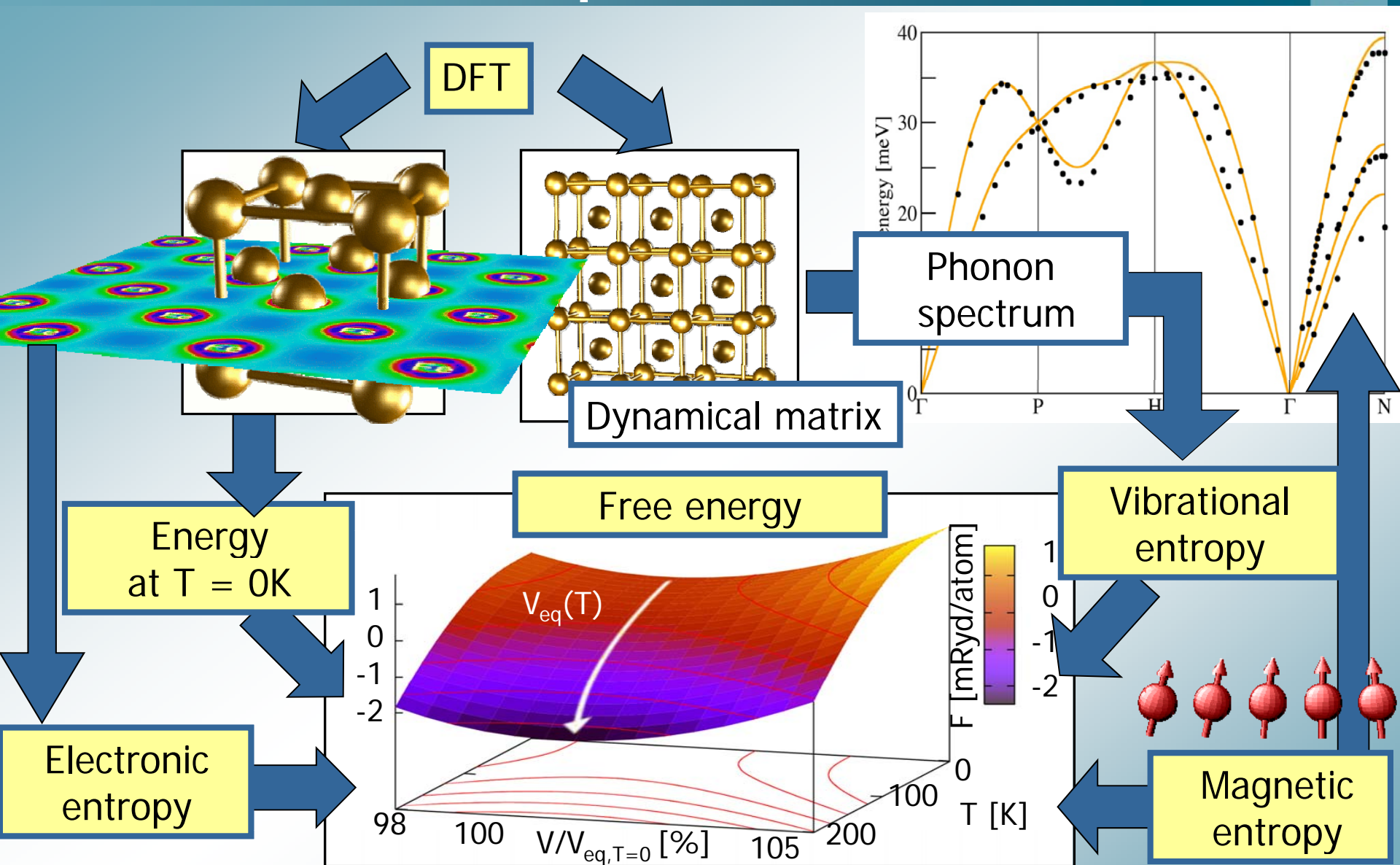


Liquidus surface



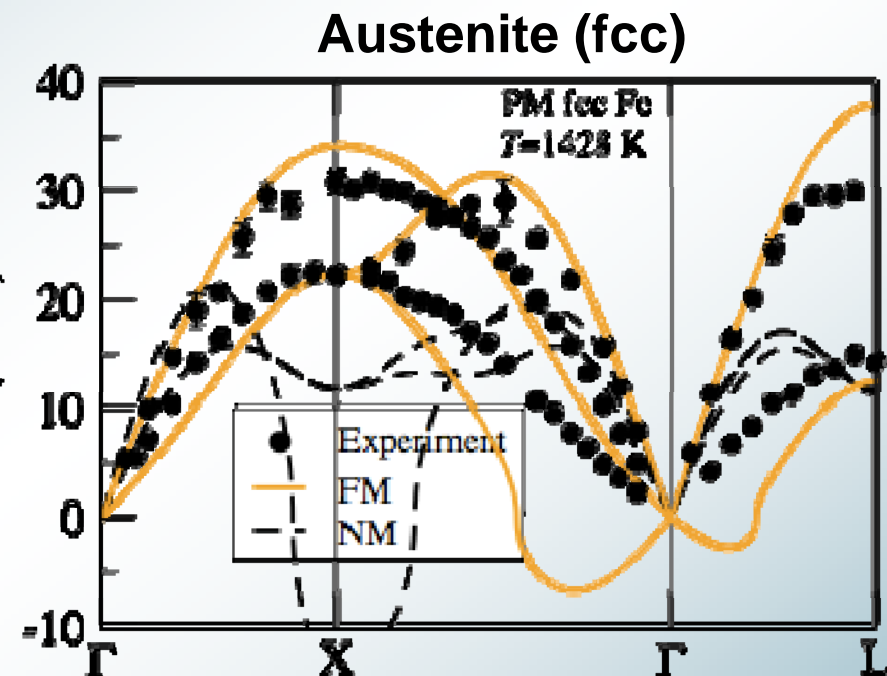
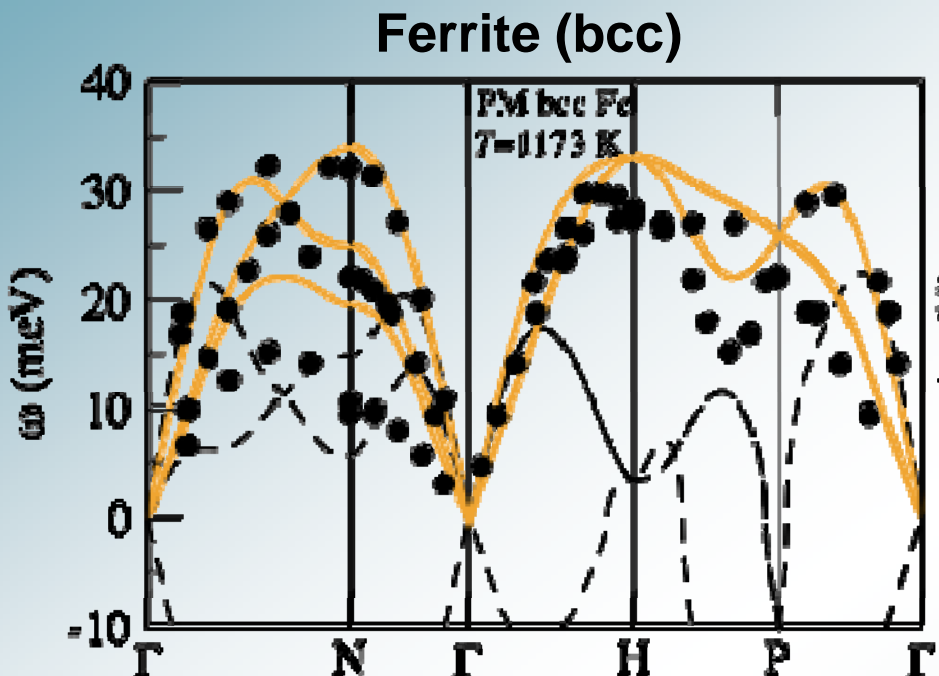
D. Djurovic, B. Hallstedt, J. v. Appen, R. Dronskowski: CALPHAD **34**, 279 (2010)

Ab initio for finite temperatures



Influence of magnetism on phonons of Fe

Phonons of iron above the Curie temperature



Spin space average (SSA) technique

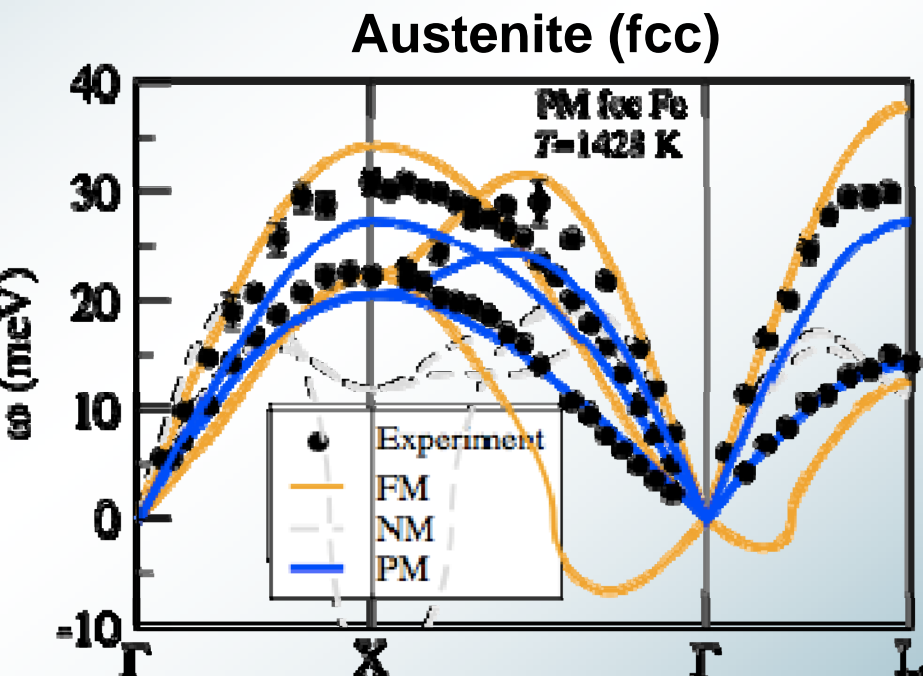
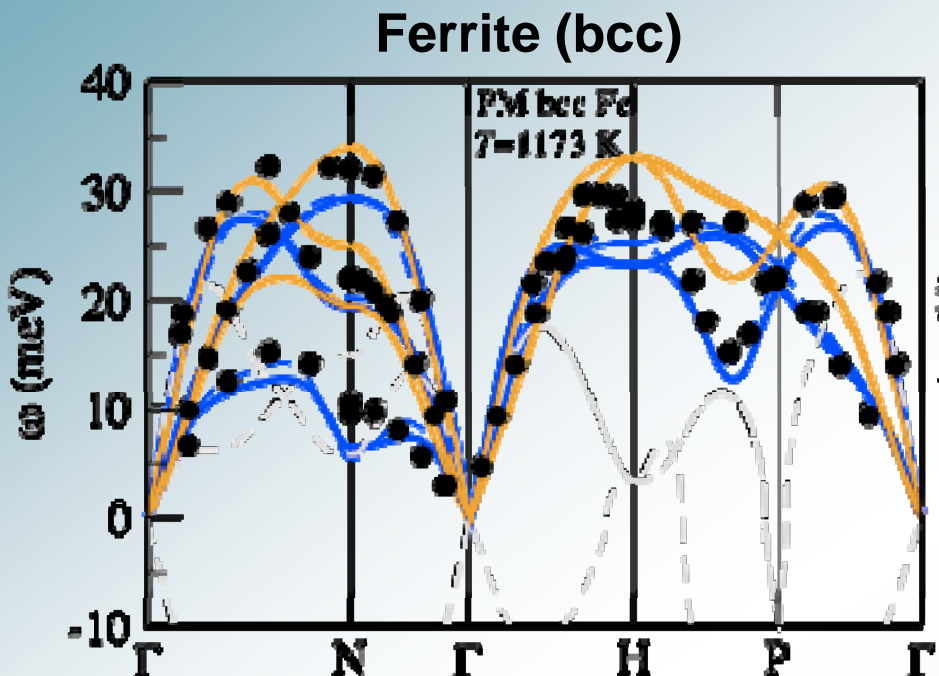
Adiabatic approximation: assuming magnetic degree of freedom faster than atomic motion, i.e. at high T each atom „feels“ same (disordered = SQS) environment



Influence of magnetism on phonons of Fe

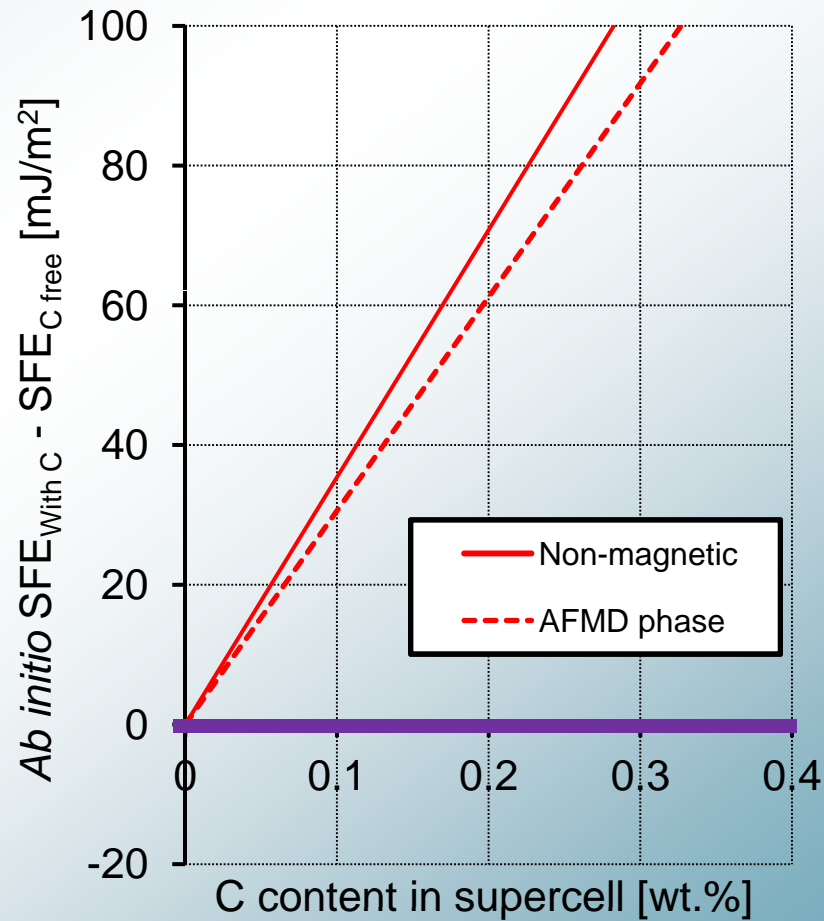
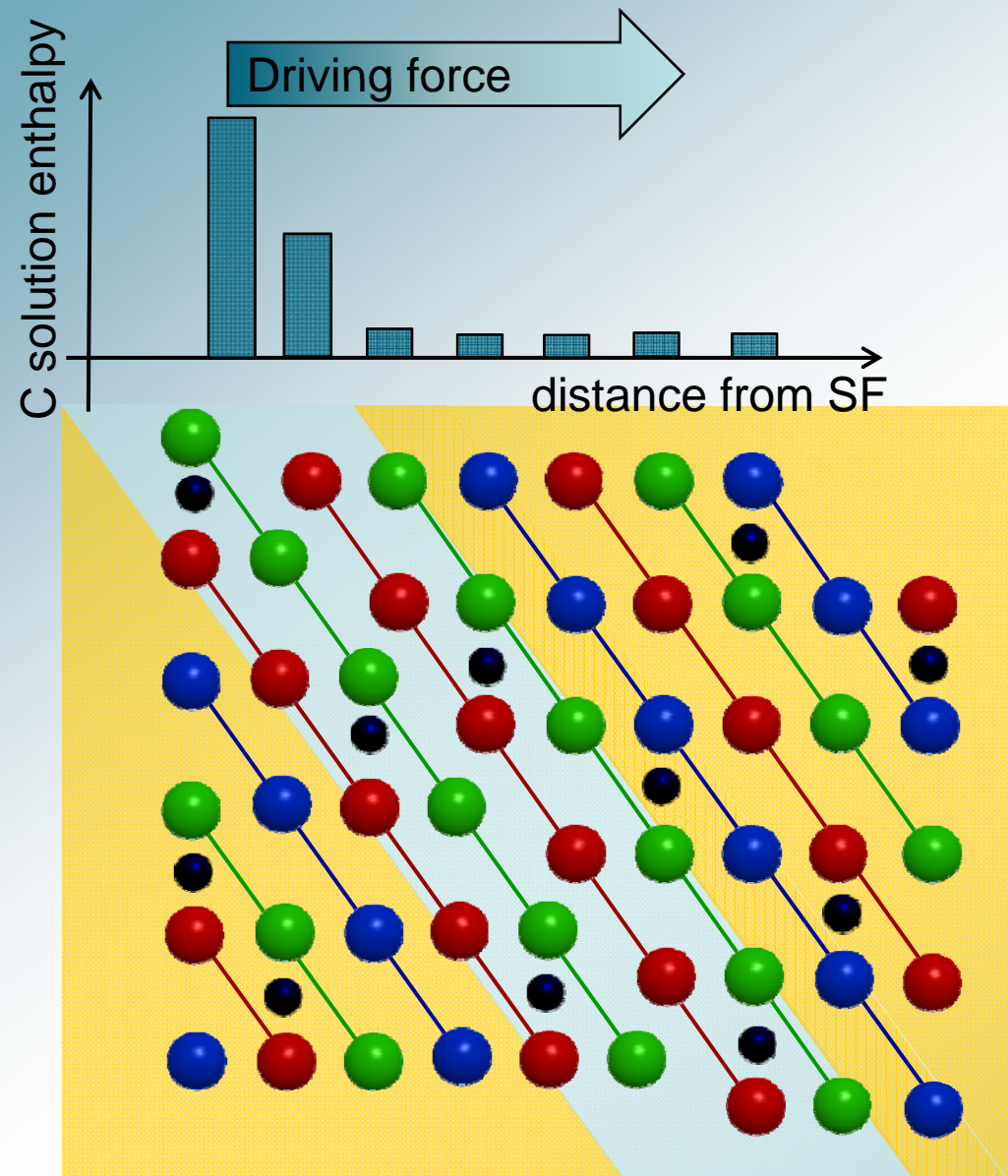


Phonons of iron above the Curie temperature

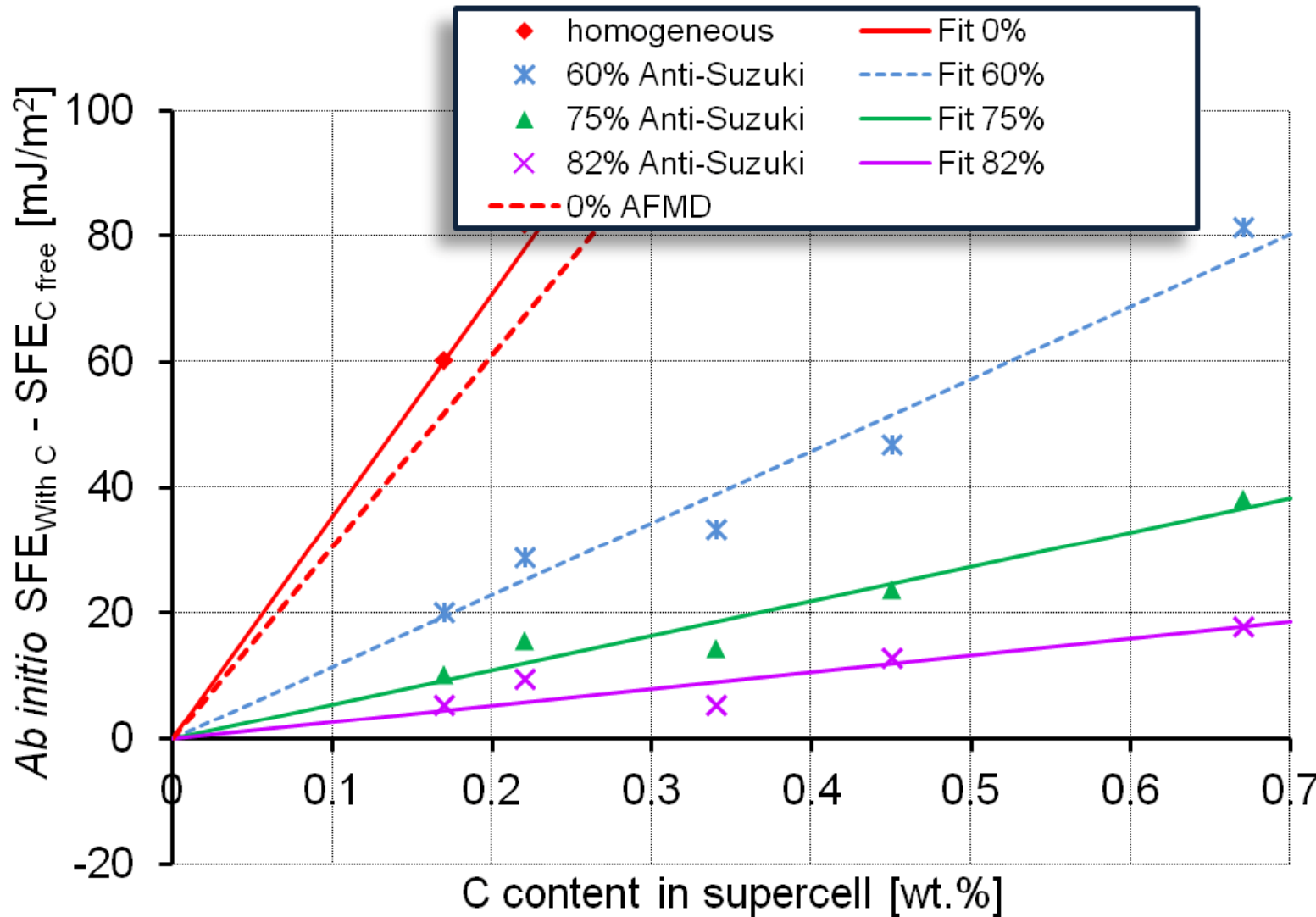


- PM calculated with newly developed spin space average (SSA) technique,
→ average over multiple spin Born-Oppenheimer surfaces
- Stability of fcc Fe due to spin excitations

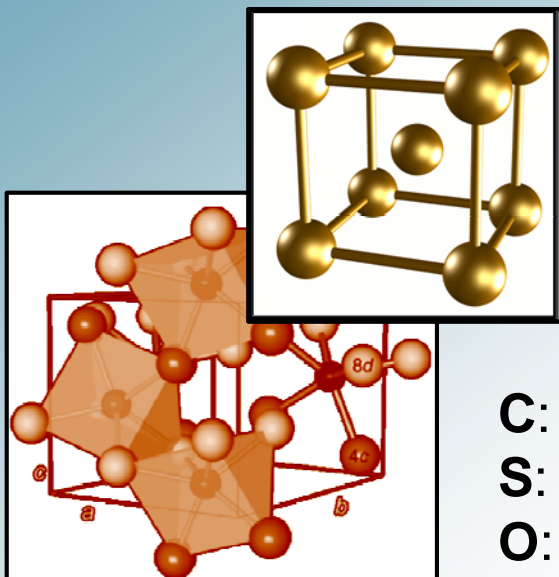
Dependence on C content



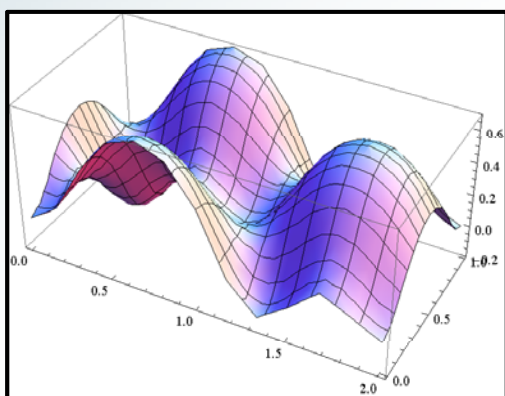
Dependence on C content



Conclusions (Challenge, Status, Outlook)



C: Small energy difference between phases
S: Quantum-effects in magnetic data
S: Phonon spectra in PM regime
O: Accurate description of phase transition



C: Strong dependence of SFE on magnetic order
S: Application to Fe-Mn alloys
O: Generalization to PM configurations